

# Progressive Myoclonus Epilepsy Caused by a Homozygous Splicing Variant of *SLC7A6OS*

Laure Mazzola, MD, PhD,<sup>1,2†</sup>  
 Karen L. Oliver, MSc,<sup>3,4,5†</sup>  
 Audrey Labalme, MSc,<sup>6</sup>  
 Betül Baykan, MD,<sup>7</sup> Mikko Muona, PhD,<sup>8,9</sup>  
 Tarja H. Joensuu, PhD,<sup>8,10</sup>  
 Carolina Courage, MD,<sup>8,10</sup>  
 Nicolas Chatron, MD, PhD,<sup>6,11</sup>  
 Giuseppe Borsani, PhD,<sup>12</sup>  
 Eudeline Alix, MSc,<sup>6</sup>  
 Francis Ramond, MD, PhD,<sup>13</sup>  
 Renaud Touraine, MD, PhD,<sup>13</sup>  
 Melanie Bahlo, PhD,<sup>4,5</sup>  
 Nerses Bebek, MD, PhD,<sup>7</sup>  
 Samuel F. Berkovic, MD, FRS <sup>3</sup>  
 Anna-Elina Lehesjoki, MD, PhD,<sup>8,10</sup> and  
 Gaetan Lesca, MD, PhD <sup>6,11</sup>

Exome sequencing was performed in 2 unrelated families with progressive myoclonus epilepsy. Affected individuals from both families shared a rare, homozygous c.191A > G variant affecting a splice site in *SLC7A6OS*. Analysis of cDNA from lymphoblastoid cells demonstrated partial splice site abolition and the creation of an abnormal isoform. Quantitative reverse transcriptase polymerase chain reaction and Western blot showed a marked reduction of protein expression. Haplotype analysis identified a ~0.85cM shared genomic region on chromosome 16q encompassing the c.191A > G variant, consistent with a distant ancestor common to both families. Our results suggest that biallelic loss-of-function variants in *SLC7A6OS* are a novel genetic cause of progressive myoclonus epilepsy.

ANN NEUROL 2021;89:402–407

**P**rogressive myoclonus epilepsies (PMEs) are a group of rare Mendelian disorders defined by the combination of action and reflex myoclonus, other types of epileptic seizures, and progressive neurocognitive impairment.<sup>1</sup> PMEs usually begin in late childhood or adolescence. Disease progression is invariable, but prognosis and longevity vary considerably according to the etiology.

There are >20 known genetic causes of PME.<sup>2</sup> They can be broadly divided into 2 clinical groups. The first

group comprises those associated with significant cognitive decline, such as Lafora disease. The second group, having relatively preserved cognition, is largely exemplified by Unverricht–Lundborg disease (ULD), caused by biallelic mutations in *CSTB*.<sup>3</sup>

Despite recent advances, a substantial proportion of PME cases remain without a molecular diagnosis, with more genetic etiologies yet to be discovered.<sup>4,5</sup> We report 2 families where multiple relatives are affected with a “ULD-like” PME phenotype and share the same rare homozygous splicing variant in *SLC7A6OS* (solute carrier family 7 member 6 opposite strand).

## Patients and Methods

### Ethical Approval and Exome Sequencing

Family 1 (Portuguese origin) was studied in a diagnostic setting and Family 2 (Turkish origin) in a research setting (Fig 1A). The institutional review board of Helsinki University Central Hospital approved the research study. Following exclusion of dodecamer repeat expansions in *CSTB*, paired-end exome sequencing (ES) was performed on 3 subjects (Family 1: IV-2; Family 2: V-4 and V-6; see Fig 1A). ES was performed on Nextseq 500 (150bp, Family 1) or HiSeq 2000 (75bp, Family 2; Illumina, San Diego, CA) following standard DNA enrichment protocols and analyzed using appropriate bioinformatic methods as previously described.<sup>6</sup>

From the <sup>1</sup>Neurology Department, Saint-Étienne University Hospital Center, Saint-Étienne, France; <sup>2</sup>Lyon Neuroscience Research Center, Lyon, France; <sup>3</sup>Epilepsy Research Centre, Department of Medicine, University of Melbourne, Austin Health, Heidelberg, Victoria, Australia; <sup>4</sup>Population Health and Immunity Division, Walter and Eliza Hall Institute of Medical Research, Parkville, Victoria, Australia; <sup>5</sup>Department of Medical Biology, University of Melbourne, Melbourne, Victoria, Australia; <sup>6</sup>Genetics Department, Lyon Civil Hospices, Lyon, France; <sup>7</sup>Departments of Neurology and Clinical Neurophysiology, Istanbul Faculty of Medicine, Istanbul University, Istanbul, Turkey; <sup>8</sup>Folkhälsan Research Center, Helsinki, Finland; <sup>9</sup>Blueprint Genetics, Helsinki, Finland; <sup>10</sup>Medicum, University of Helsinki, Helsinki, Finland; <sup>11</sup>NeuroMyoGene Institute, University of Lyon, Claude Bernard University Lyon 1, Lyon, France; <sup>12</sup>University of Brescia, Brescia, Italy; and <sup>13</sup>Genetics Department, Saint-Étienne University Hospital Center, Saint-Étienne, France

Address correspondence to Dr Lesca, Laboratoire de Cytogénétique, Centre de Biologie et de Pathologie Est, Groupement Hospitalier Est, 59 Boulevard Pinel, 69677 Bron, France. E-mail: gaetan.lesca@chu-lyon.fr

Additional supporting information can be found in the online version of this article.

Received Jul 2, 2020, and in revised form Oct 17, 2020. Accepted for publication Oct 19, 2020.

View this article online at wileyonlinelibrary.com. DOI: 10.1002/ana.25941.

<sup>†</sup>L.M. and K.L.O. are equal first authors.

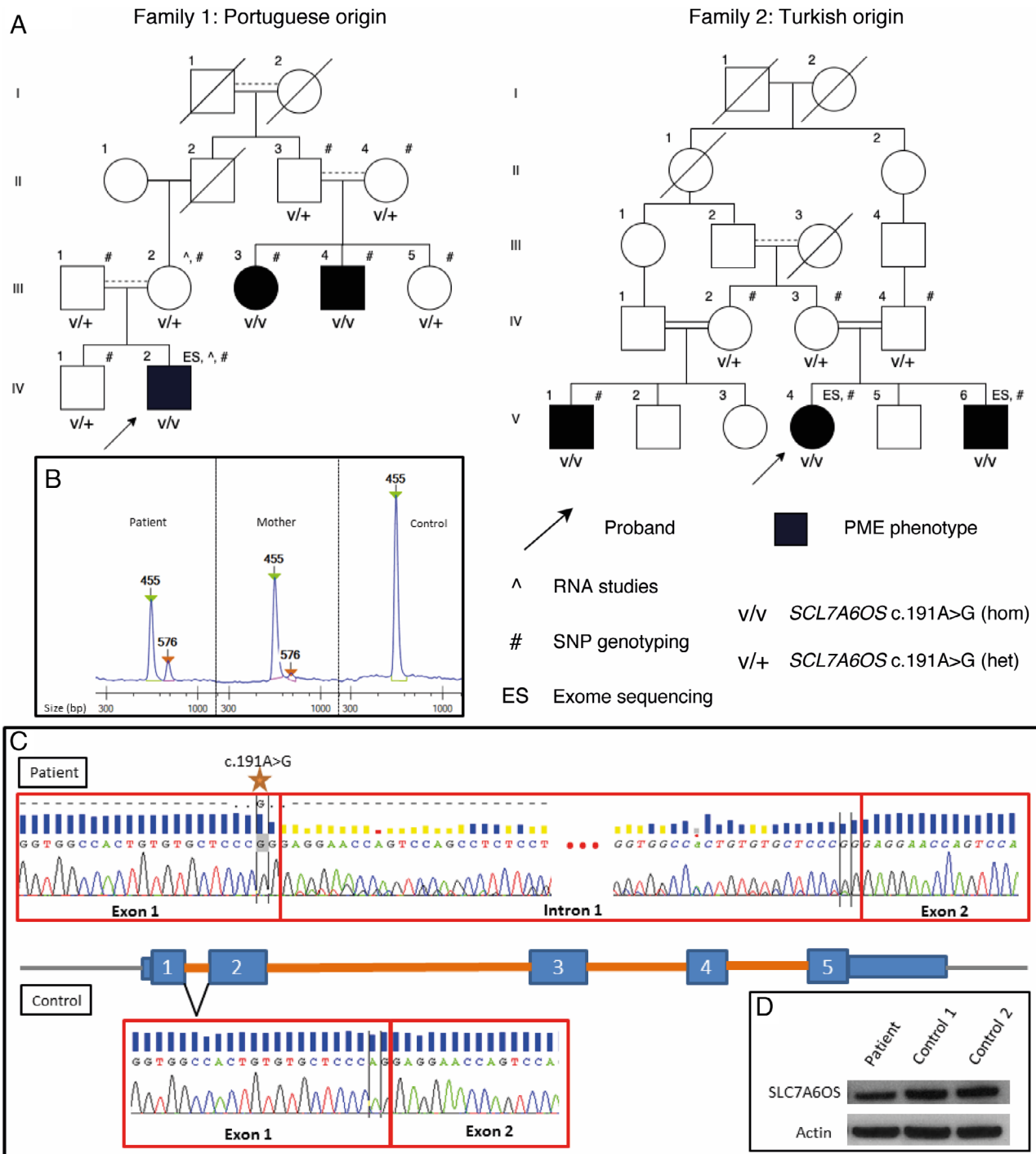


**FIGURE 1:** (A) Family pedigrees showing *SLC7A6OS* variant segregation and the type of genetic study performed in each subject. Consanguineous parental unions are indicated with 2 connecting lines. Consanguinity was not reported by the members of Family 1; however, the families were from the same rural area, and a common ancestor had been hypothesized. Subsequent inbreeding coefficient calculations supported the consanguineous unions as depicted by the dotted lines. (B) Migration on a Labchip GX of polymerase chain reaction products obtained by amplification of exons 1 to 3 of blood-derived *SLC7A6OS* cDNA. The expected fragment of 455bp was obtained for the 3 individuals tested (Patient III-2 in Family 1, his mother, and a control). For the patient and his mother, an additional 576bp amplicon was detected, representing, respectively, approximately 20% or 10% of the amount of *SLC7A6OS* cDNA, with the expected fragment decreasing in proportion. (C) Sanger sequencing of both the 455 and 576bp amplicons. The "abnormal" transcript corresponds to the retention of the complete intron 1 (+121bp). (D) In Western blot analysis, a decrease in the abundance of the *SLC7A6OS* protein was detected in the patient (III-2, Family 1) compared to controls. The analysis was performed in duplicates with 2 deposits each time. Mean estimations with a ChemiDoc imager were about 50% of the expression in controls. [Color figure can be viewed at [www.annalsofneurology.org](http://www.annalsofneurology.org)]

### Expression Studies in Family 1

Blood-derived RNA samples were collected from the affected proband (IV-2) and his unaffected mother (III-2). cDNA was synthesized by standard techniques.<sup>7</sup> Primers specific for “wild-type” *SLC7A6OS* transcript were used for real-time polymerase chain reaction (PCR): ex1/2F, TCCCAGGAGGAACCAGTCCA and ex2R, TCAGGT TCTCCCTCCTCGTG.

Proteins were extracted from lymphoblastoid cells. Forty micrograms of each sample was electrophoresed on NuPAGE 12% Bis-Tris Protein Gels (ThermoFisher Scientific, Waltham, MA) and transferred to Hybond-ECL Nitrocellulose membrane (GE Healthcare, Velizy-Villacoublay, France). The membrane was incubated overnight with primary antibodies: rabbit polyclonal anti-*SLC7A6OS* (ab122727; Abcam, Cambridge, UK) used at dilution of 1:250 or rabbit monoclonal antiactin antibody SAB5500001, clone SP124, (Sigma-Aldrich, Saint Louis, MO) used at 1:1,000 in 0.1% phosphate-buffered saline (PBS)-Tween with 3% milk. After washing, the membrane was incubated for 1 hour at room temperature with secondary antibodies: donkey antirabbit IgG H&L (horseradish peroxidase; ab16284) in PBS with 3% milk. Blots were revealed by ECL Prime kit (Pierce, Woburn, MA). The chemiluminescent signals of blots were quantified using a ChemiDoc imager (Bio-Rad, Marnes-la-Coquette, France).

### Post Hoc Linkage and Haplotype Analyses

Nine family members from Family 1 and 6 from Family 2 were single nucleotide polymorphism (SNP) genotyped (see Fig 1A). Pairwise sample identity-by-descent (IBD) analyses were performed using KING,<sup>8</sup> and inbreeding coefficients were estimated by FEstim.<sup>9</sup> Autosomal recessive linkage analyses were performed using MERLIN.<sup>10</sup> Genotyped SNPs were manually interrogated to verify linkage breakpoints and determine haplotype lengths and sharing. Copy number variants (CNVs) were detected using PennCNV.<sup>11</sup>

### Brain Coexpression Exploratory Analysis

Gene coexpression analyses were performed using normalized developing brain expression data from BrainSpan (<http://www.brainspan.org/>). Genes were removed if they had expression values missing from >50% of samples or expression variation of <0.5 across all samples. A total of 15,957 genes, across 71 samples, remained in the filtered dataset. Using log<sub>2</sub>-transformed expression values, a matrix of weighted pairwise gene correlations was generated; weights were determined by  $1/\sqrt{n}$ , where  $n$  is the number of samples contributed by the respective individual.

## Results

### Clinical Presentation of Patients

The clinical features of all 6 patients were similar and, in the early course of disease, resembled classic ULD (Table ). Electroencephalographic recordings showed relative preservation of background rhythms with generalized polyspike, polyspike-wave, and sometimes spike-wave discharges. Discharges were enhanced during hyperventilation and photic stimulation. Giant somatosensory evoked potentials were documented in patients from both families (Family 1: IV-2, Family 2: V-1). Brain magnetic resonance imaging at disease onset was normal (Family 1: IV-2, Family 2: V-6 and V-1), with serial studies in Family 2 demonstrating deterioration to marked cerebellar (V-6) and cerebral atrophy (V-1).

### Exome Analysis Prioritizes *SLC7A6OS* Variant

Autosomal recessive modes of inheritance were hypothesized based on pedigree structure (see Fig 1A). Loss-of-function variants, including predicted splicing variants, were further prioritized. This approach led to the homozygous *SLC7A6OS* NM\_032178.2: c.191A > G substitution being identified as the most likely pathogenic variant in both families (see Supplementary Table S1). Pedigree segregation supported the variant being disease-causing in the homozygous state (see Fig 1A).

### Patient RNA and Protein Expression Studies

The *SLC7A6OS* c.191A > G affects the second last nucleotide of the first exon. Splicing prediction tools predicted abolition of the donor site (see Supplementary Table S1). Analysis of cDNA amplicons from exon 1 to exon 3 showed a single expected product of 455bp in controls (see Fig 1B). In Patient IV-2 and his mother III-2 (Family 1), the normal 455bp product was decreased in amount and there was an additional product of 576bp (see Fig 1B, C), resulting from the retention of the intron 1 (121bp), expected to lead to a frameshift.

Quantification of *SLC7A6OS* transcripts by quantitative reverse transcriptase polymerase chain reaction in Patient IV-2 revealed that expression of *SLC7A6OS* in blood was approximately 60% and in lymphoblastoid cells approximately 15% of that in controls. In the blood of the heterozygous mother (III-2), the *SLC7A6OS* expression was approximately 85% of controls. *SLC7A6OS* protein expression was also markedly reduced (see Fig 1D).

### Post Hoc Linkage and Haplotype Analysis

Inbreeding estimates were consistent with consanguinity in both families (see Fig 1A). Under an autosomal recessive disease model, a single genome-wide significant linkage peak (logarithm of odds [LOD] > 3.0) was found for

**TABLE. Clinical Presentation and Summary of Affected Individuals from Both Families with the c.191A > G Variant in *SLC7A6OS***

Patient ID	Family 1			Family 2		
	III-3	III-4	IV-2	V-1	V-4	V-6
Sex	F	M	M	M	F	M
Development	Normal	Normal	Normal	Mild psychomotor delay <sup>a</sup>	Normal	Normal
Age at onset	21 yr	17 yr	11 yr	12 yr <sup>b</sup>	13 yr	11 yr <sup>c</sup>
First symptom	TCS	TCS	Myoclonus	TCS	Myoclonus	TCS
Myoclonus	+++	+++	+++	+++	++	++
TCS	+	+	+	+	—	+
Cerebellar signs	Ataxia	Ataxia	Ataxia, dysarthria, dysmetria	Ataxia, dysarthria, dysmetria	Ataxia, dysarthria, dysmetria	Ataxia, dysarthria
Cognitive decline; dysfunction	No	No	Yes, mild; visual perception and attentional dysfunction	Yes, mild; spatial recognition and attentional dysfunction	No	Yes, mild; attentional dysfunction
Outcome (age)	Wheelchair (22 yr); living (41 yr)	Wheelchair (21 yr); living (38 yr)	Wheelchair (17 yr); living (22 yr)	Wheelchair mostly (30); living (32 yr)	Limited ambulation; living (42 yr)	Limited ambulation; living (43 yr)
Antiseizure drugs	CNZ, LRZ, LEV, VPA	CNZ, DZP, LEV, VPA	VPA, LEV, CLB, TPM, PRIM	VPA, LEV, ZNS	PHT, <sup>d</sup> VPA, CNZ	VPA, CNZ
Other diagnoses	Depression (mild)	Depression (mild); addiction (drugs and alcohol)	—	Type 1 diabetes; mild diabetic retinopathy; anxiety	—	Attention-deficit disorder

<sup>a</sup>Walking acquired after the age of 2 years.<sup>b</sup>Febrile seizure at 1 year.<sup>c</sup>Possible afebrile seizure at the age of 1.5 years and poor balance noted at 9 years.<sup>d</sup>Symptom aggravation.

+ = mild; ++ = moderate; +++ = severe; — = not observed; CLB = clobazam; CNZ = clonazepam; DZP = diazepam; F = female; LEV = levetiracetam; LRZ = lorazepam; M = male; PHT = phenytoin; PRIM = primidone; TCS = tonic-clonic seizures; TPM = topiramate; VPA = valproate; ZNS = zonisamide.

both families on chromosome 16. No other regions with an LOD score of >0.5 were identified. The homozygous *SLC7A6OS* variant is located at chr16:68,344,639bp (86.6cM); both linkage regions include this base position (hg19; Fig 2A). No CNVs were detected in the linkage region for either family.

No close genetic relatedness between the 2 families was revealed by IBD analysis (third-degree relatives reliably excluded). However, to explore whether the variant may have arisen from a distant common ancestor, we compared

the c.191A > G variant haplotype in both families. A total of 135 consecutive SNPs were shared by the 2 families at locus chr16q22.1 (chr16: 67,670,682–68,548,709; see Fig 2B). The shared haplotype is ~880kb (~0.85cM) in length, consistent with a founder effect.

### Brain Coexpression Exploratory Analysis

We explored brain coexpression patterns between *SLC7A6OS* and genes already known to cause an “ULD-like” PME phenotype (ie, *CSTB*, *KCNK1*, *GOSR2*,

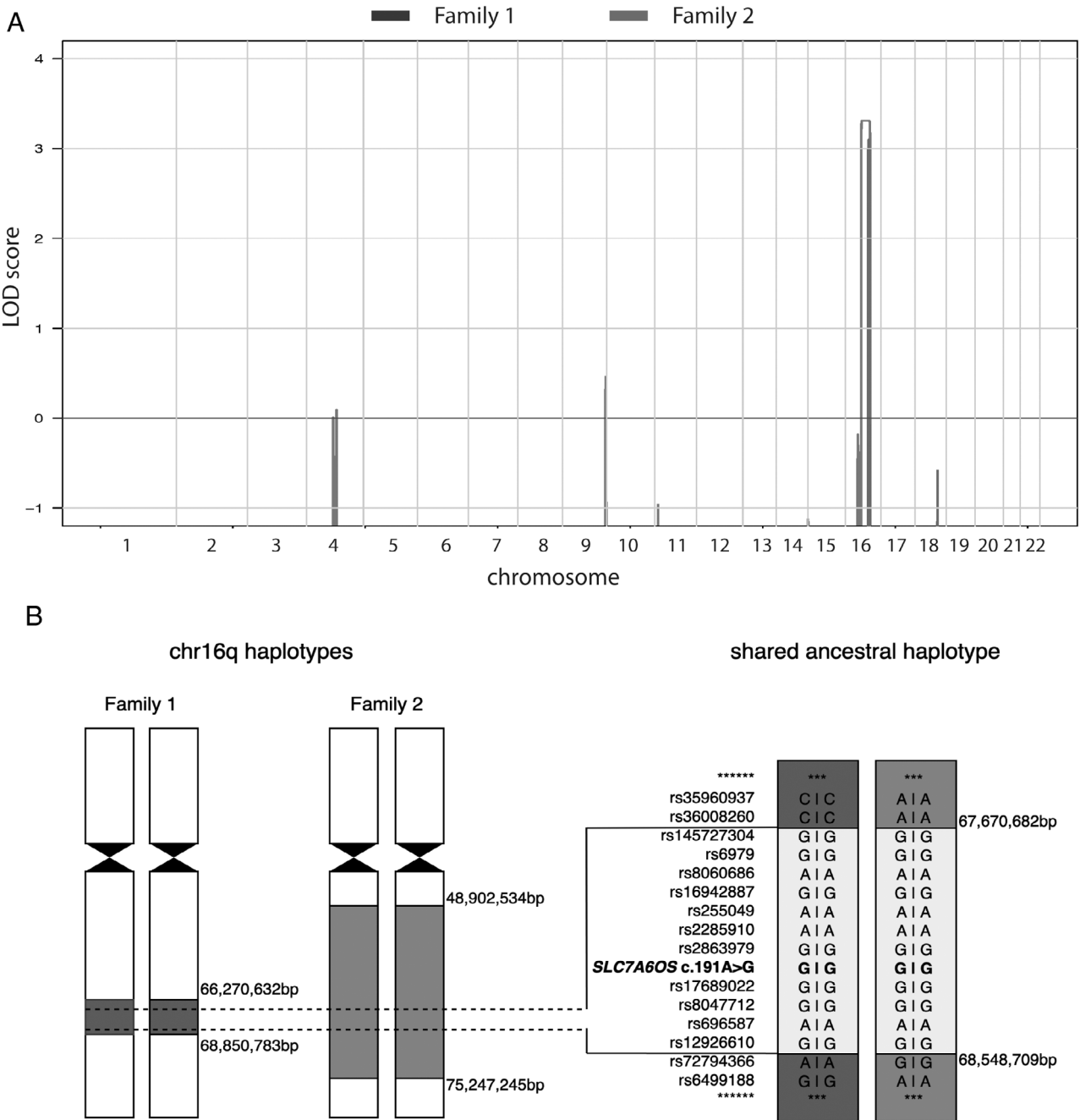


**FIGURE 2:** (A) Genome-wide parametric linkage logarithm of odds (LOD) scores for Family 1 (dark gray) and Family 2 (light gray) under an autosomal recessive disease model. (B) Chr16q haplotypes for each family demonstrating the run of homozygosity on either side of the *SLC7A6OS* c.191A > G variant in dark gray (Family 1) and light gray (Family 2). The ancestral chr16q22.1 haplotype shared by both families is represented by a small selection of markers from the list of 135 consecutively shared single nucleotide polymorphisms.

*SCARB2*, *ASAHI*, *CERS1*).<sup>2</sup> The analysis revealed that *SLC7A6OS* and *SCARB2* are in the top 5% of the most highly coexpressed genome-wide genes in the developing brain; *SLC7A6OS* and *GOSR2* are in the top 10%. With *ASAHI*, the 4 genes form a set of significantly positively correlated genes that all negatively correlate with *CERS1* ( $p < 0.01$ , Monte Carlo sampling).

**Discussion**

We describe 2 unrelated families with PME and an identical homozygous variant affecting the splicing of *SLC7A6OS*. The similar phenotypic presentation of the 6 patients, combined with a likely founder effect origin of the variant, strongly suggests that it is the underlying cause of PME for these patients. Whereas the clinical and

electrophysiological presentation was similar to ULD,<sup>3,12</sup> onset age was slightly later (11–21, mean = 14 years) and progression with loss of ambulation and cognitive decline was faster than typical for ULD.

The c.191A > G variant was predicted to disrupt an *SLC7A6OS* donor splice site and patient cDNA, and protein studies confirmed this. We observed the production of an abnormal isoform with the retention of intron 1. Expression of *SLC7A6OS* in blood was approximately 60% and in lymphoblastoid cells approximately 15% of that in controls. Expression of the normal *SLC7A6OS* isoform was markedly reduced, which was confirmed by a decrease of ~50% of the *SLC7A6OS* protein product.

The exact function of *SLC7A6OS* remains unknown, although there is some evidence to support it playing a role in RNA polymerase II nuclear import.<sup>13</sup> In the zebrafish, *slc7a6os* is highly expressed in the central nervous system (CNS) during development.<sup>14</sup> Furthermore, functional knockdown of *slc7a6os* by splice-blocking morpholinos showed morphological defects in the CNS and reduced mobility. Interestingly, the morpholino used by Benini and colleagues<sup>14</sup> targets the *slc7a6os* exon1–intron1 boundary and is expected to cause the retention of intron 1 in the mature mRNA, thus mimicking the effect of the c.191A > G variant in our PME patients.

To further support the role of *SLC7A6OS* in PME, we compared its coexpression patterns in the developing human brain with established “ULD-like” disease genes. Our analysis identified *SCARB2* as the established “ULD-like” gene, with the most highly correlated brain coexpression pattern with *SLC7A6OS*, and that together with *GOSR2*, *ASAH1*, and *CERS1* they form a cluster of significantly coexpressed genes. With a putative role for *SLC7A6OS* in nuclear import, all 5 genes are broadly involved in intracellular trafficking, with correlated coexpression signatures supporting a potential shared pathway in the brain specifically.

In conclusion, these data suggest that biallelic variants in *SLC7A6OS*, displaying a founder effect, are a rare, new cause of PME, with a phenotype similar to ULD.

## Acknowledgments

This work was supported by the Victorian Government’s Operational Infrastructure Support Program and the National Health and Medical Research Council Independent Research Institute Infrastructure Support Scheme.

We thank the patients from both families for their participation to the study; Dr I. Rouvet and the Centre

for Cell Biology for the production of lymphoblastoid cells; and Drs A. Fourier, R. Menassa, and P. Hakala for technical assistance.

## Author Contributions

Conception and design of the study: G.L., A-E.L., S.F.B., M.B. Acquisition and analysis of data: all authors. Drafting a significant portion of the manuscript or figures: L.M., K.L.O., A.L., S.F.B., A-E.L., G.L.

## Potential Conflicts of Interest

Nothing to report.

## References

1. Marseille Consensus Group. Classification of progressive myoclonus epilepsies and related disorders. *Ann Neurol* 1990;28:113–116.
2. Orsini A, Valetto A, Bertini V, et al. The best evidence for progressive myoclonic epilepsy: a pathway to precision therapy. *Seizure* 2019;71:247–257.
3. Kalviainen R, Khyuppenen J, Koskenkorva P, et al. Clinical picture of EPM1-Unverricht-Lundborg disease. *Epilepsia* 2008;49:549–556.
4. Franceschetti S, Michelucci R, Canafoglia L, et al. Progressive myoclonic epilepsies: definitive and still undetermined causes. *Neurology* 2014;82:405–411.
5. Muona M, Berkovic SF, Dibbens LM, et al. A recurrent de novo mutation in KCNC1 causes progressive myoclonus epilepsy. *Nat Genet* 2015;47:39–46.
6. Kinay D, Oliver KL, Tuzun E, et al. Evidence of linkage to chromosome 5p13.2-q11.1 in a large inbred family with genetic generalized epilepsy. *Epilepsia* 2018;59:e125–e129.
7. Schluth-Bolard C, Diguët F, Chatron N, et al. Whole genome paired-end sequencing elucidates functional and phenotypic consequences of balanced chromosomal rearrangement in patients with developmental disorders. *J Med Genet* 2019;56:526–535.
8. Manichaikul A, Mychaleckyj JC, Rich SS, et al. Robust relationship inference in genome-wide association studies. *Bioinformatics* 2010;26:2867–2873.
9. Leutenegger AL, Labalme A, Genin E, et al. Using genomic inbreeding coefficient estimates for homozygosity mapping of rare recessive traits: application to Taybi-Linder syndrome. *Am J Hum Genet* 2006;79:62–66.
10. Abecasis GR, Cherny SS, Cookson WO, Cardon LR. Merlin—rapid analysis of dense genetic maps using sparse gene flow trees. *Nat Genet* 2002;30:97–101.
11. Wang K, Li M, Hadley D, et al. PennCNV: an integrated hidden Markov model designed for high-resolution copy number variation detection in whole-genome SNP genotyping data. *Genome Res* 2007;17:1665–1674.
12. Canafoglia L, Ferlazzo E, Michelucci R, et al. Variable course of Unverricht-Lundborg disease: early prognostic factors. *Neurology* 2017;89:1691–1697.
13. Czeko E, Seizl M, Augsberger C, et al. Iwr1 directs RNA polymerase II nuclear import. *Mol Cell* 2011;42:261–266.
14. Benini A, Cignarella F, Calvarini L, et al. *slc7a6os* gene plays a critical role in defined areas of the developing CNS in zebrafish. *PLoS One* 2015;10:e0119696.